

In Utero Gene Therapy Rescues Vision in a Murine Model of Congenital Blindness

Nadine S. Dejneka,^{1,*} Enrico M. Surace,^{1,*} Tomas S. Aleman,¹
Artur V. Cideciyan,¹ Arkady Lyubarsky,¹ Andrey Savchenko,¹
T. Michael Redmond,² Waixing Tang,¹ Zhangyong Wei,¹ Tonia S. Rex,¹
Ernest Glover,¹ Albert M. Maguire,¹ Edward N. Pugh Jr.,¹
Samuel G. Jacobson,¹ and Jean Bennett^{1,†}

¹F.M. Kirby Center and Scheie Eye Institute, Department of Ophthalmology, University of Pennsylvania, 51 N. 39th Street, Philadelphia, PA 19104-2689, USA

²Laboratory of Retinal Cell and Molecular Biology, National Eye Institute, National Institutes of Health, 6 Center Drive, MSC 2740, Bethesda, MD 20892-2740, USA

*These authors contributed equally to this work.

†To whom correspondence and reprint requests should be addressed. Fax: (215) 573-7155. E-mail: jebennet@mail.med.upenn.edu.

The congenital retinal blindness known as Leber congenital amaurosis (LCA) can be caused by mutations in the *RPE65* gene. *RPE65* plays a critical role in the visual cycle that produces the photosensitive pigment rhodopsin. Recent evidence from human studies of LCA indicates that earlier rather than later intervention may be more likely to restore vision. We determined the impact of *in utero* delivery of the human *RPE65* cDNA to retinal pigment epithelium cells in a murine model of LCA, the *Rpe65*^{-/-} mouse, using a serotype 2 adeno-associated virus packaged within an AAV1 capsid (AAV2/1). Delivery of AAV2/1-CMV-*hRPE65* to fetuses (embryonic day 14) resulted in efficient transduction of retinal pigment epithelium, restoration of visual function, and measurable rhodopsin. The results demonstrate AAV-mediated correction of the deficit and suggest that *in utero* retinal gene delivery may be a useful approach for treating a variety of blinding congenital retinal diseases.

Key Words: adeno-associated virus, retinal degeneration, retina, mouse model, gene therapy, neurodegeneration, *in utero* therapy, viral gene transfer, genetic disease, phototransduction

INTRODUCTION

Leber congenital amaurosis (LCA) is a genetically heterogeneous disorder that causes severe visual deficits in infants [1]. About 10% of LCA is caused by mutations in the gene encoding *RPE65* [2,3]. *RPE65* is a highly conserved 61-kDa protein (previously thought to be 65 kDa) that is primarily expressed in the microsomal membrane fraction of the retinal pigment epithelium (RPE). Characteristically, the visual cycle in *Rpe65*^{-/-} mice is blocked, and these animals are not able to produce biochemically detectable 11-*cis*-retinal. Consequently, rhodopsin regeneration is impaired, resulting in severely abnormal retinal function [4].

RPE65 expression is developmentally regulated. In rats, *Rpe65* message is detected as early as embryonic day (E) 18 and protein is evident between postnatal days (P) 4 and 5, persisting throughout adulthood [5]. While *Rpe65*^{-/-} mice exhibit severe and early impair-

ment of retinal function, there is a gross preservation of retinal structure. Nevertheless, there are some early microscopic abnormalities, including the presence of RPE inclusions during the first week of birth, shorter and disorganized rod outer segments at 1 month of age, and significantly reduced levels of opsin compared to wild-type animals [4,6]. *RPE65* is also strongly expressed in the human fetal eye. Evidence is mounting that the human retinal disease resulting from *RPE65* mutations may be more aggressive than murine or canine models. Retinal histological abnormalities were present in an aborted fetus with an *RPE65* mutation [7] and retinal thinning has been documented in 12- and 13-year-old LCA patients with *RPE65* mutations [8]. While LCA patients can frequently retain some useful visual function through adolescence [9], early intervention may be necessary to correct the disease phenotype fully. In the present

study, we have tested the efficacy of the earliest possible intervention—*in utero* intervention. In additional cohorts, we administered treatments during the first months of postnatal life. The results demonstrate that both fetal and early postnatal intervention can correct the LCA phenotype.

RESULTS

In Utero and Postnatal Retinal Gene Therapy: No Impairment of Development or Growth

We introduced AAV2/1-CMV-*hRPE65* into fetal (E14) and young adult (P30 and P75) *Rpe65*^{-/-} mice as shown in the time line (Fig. 1a). During the period under study, the eye undergoes dramatic growth and the retina transforms from a homogeneous-appearing group of progenitor cells to a laminated structure containing many different specialized retinal cell types. (Figs. 1b and 1c). Each animal received a single subretinal injection of AAV2/1-CMV-*hRPE65* in one eye. The contralateral eye was left untouched (fetus) or received a subretinal injection of phosphate-buffered saline (PBS; adult).

For the *in utero* studies, we injected 52 fetuses in 12 operations. Thirty-one pups were delivered without complications and 13 survived to adulthood. (The pups that did not survive to adulthood were neglected and cannibalized by foster mothers.) The surviving animals devel-

oped normally, and the eyes/retinas had no apparent macroscopic or microscopic abnormalities.

RPE65 Expression after *in Utero* AAV2/1-Mediated Retinal Gene Therapy

Following fetal subretinal delivery of virus, we detected RPE65 immunohistochemically on P0 in the RPE (Fig. 2a) and RPE65 persisted throughout the course of the studies (through age 5–6 months). Immunohistochemical findings shown in Fig. 2b represent the 3-month time point. Adult administration of virus also resulted in stable transduction of RPE (data not shown). We did not detect RPE65 protein in untreated or control-injected *Rpe65*^{-/-} retinas (Fig. 2c).

Improvement of Retinal Function after *in Utero* Gene Therapy

We assayed retinal function with electroretinography (ERG) 1–2 months after subretinal injections of AAV2/1-CMV-*hRPE65* delivered *in utero* ($n = 13$) or at the postnatal age of 1–2.5 months ($n = 30$). ERG waveforms from the two eyes (Eye 1, Eye 2) of a representative 2-month-old *Rpe65*^{-/-} mouse injected *in utero* at E14 exemplify the treatment effect (Figs. 3a and 3b). ERGs in Eye 2 (defined below) resemble normal responses (Fig. 3a, left) with a near-normal threshold of $-2.9 \log \text{scot-cd s m}^{-2}$ (ERG b-wave thresholds for *Rpe65*^{+/+}, -3.9 ± 0.3

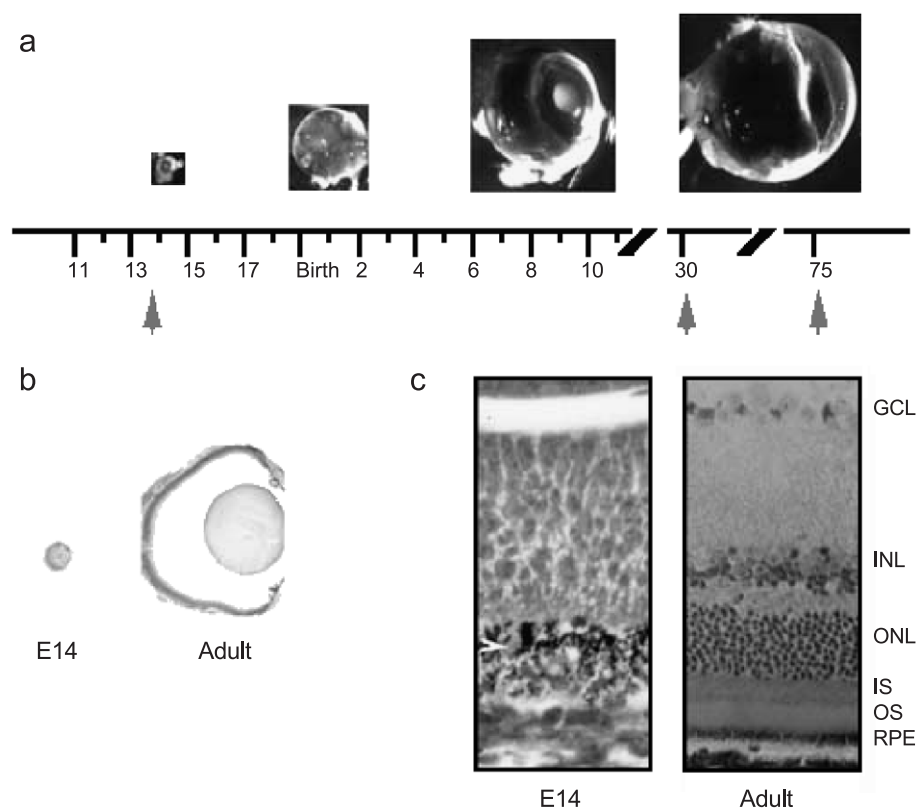
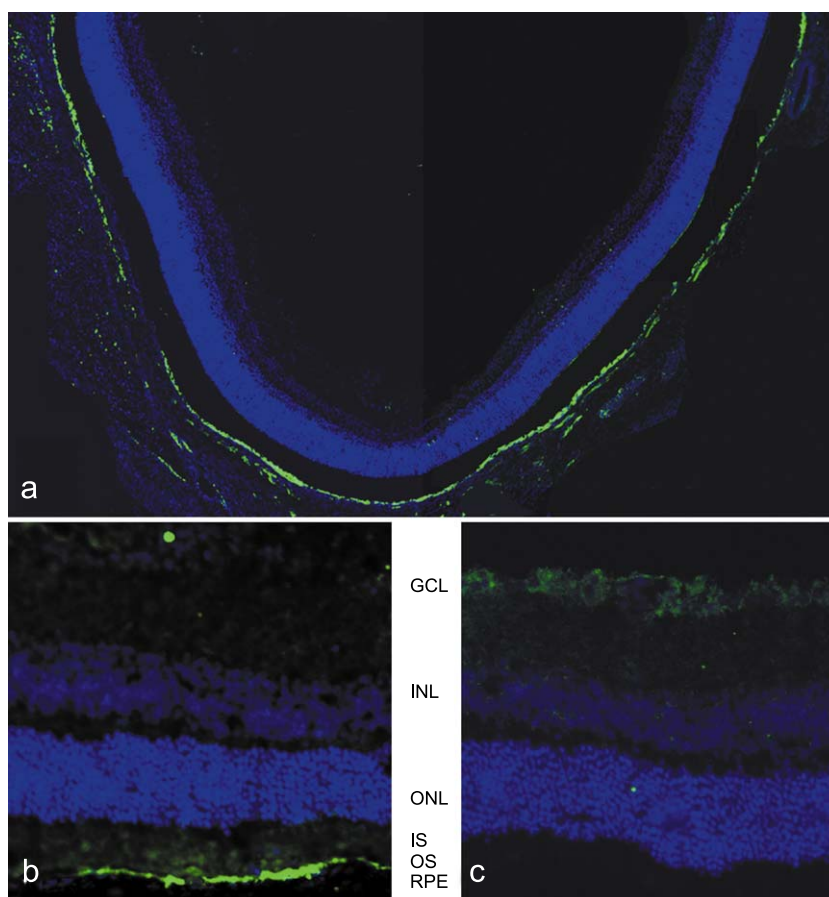


FIG. 1. Change in size and retinal lamination of the mouse eye with age. The volume/surface of the eye increase dramatically over the course of development. (a) For size perspective, globes of C57BL/6 mice are shown at E14, P1, P7, and adulthood (P30, P75). AAV2/1-CMV-*hRPE65* was administered to animals on E14, P30, and P75 (arrows). Corresponding histology at (b) low magnification and (c) higher magnification shows the undifferentiated retinal progenitor cells at E14 and the lamination of the mature retina. RPE, retinal pigment epithelium; OS, outer segments of the photoreceptors; IS, inner segments; ONL, outer nuclear layer; INL, inner nuclear layer; GCL, ganglion cell layer. Arrowhead indicates position of the RPE. Original magnifications: a and b, 11.7 \times ; c, E14, 40 \times , adult, 20 \times .

FIG. 2. RPE65 protein is detected immunohistochemically in retinas of *Rpe65*^{-/-} animals treated with AAV2/1-CMV-*hrRPE65*. (a) RPE65 protein (green label) is detected in the RPE as early as P0 following administration of vector to the fetal retina (E14). (b) Adult retina injected with AAV2/1-CMV-*hrRPE65* *in utero* and evaluated 3 months posttreatment. (c) Contralateral (control) eye to that shown in (b). There is no detectable RPE65 protein in (c). Similar RPE expression profiles were seen when animals were injected postnatally (not shown). Original magnifications: (a) Composite of photos taken at 5 \times , (b and c) 20 \times . RPE, retinal pigment epithelium; OS, outer segment layer; IS, inner segment layer; ONL, outer nuclear layer; INL, inner nuclear layer; GCL, ganglion cell layer.



log scot-cd s m⁻², *n* = 6). In contrast, Eye 1 has barely recordable responses to these light stimuli, with a threshold of -0.5 log scot-cd s m⁻², similar to uninjected *Rpe65*^{-/-} mice (-0.6 ± 0.3 log scot-cd s m⁻², *n* = 8). The ERG b-wave threshold improvement in Eye 2 is likely

due to a substantial increase in rod photoreceptor sensitivity, as demonstrated with photoresponses in the same mouse (Fig. 3b). Eye 2 shows a fast photoresponse leading edge (peaking near 4 ms) with a near-normal sensitivity of 3.39 log scot-cd⁻¹ m² s⁻³ (sensitivity for *Rpe65*^{+/+}, 3.2

FIG. 3. Improvement of retinal function by gene therapy in *Rpe65*^{-/-} mice *in utero*. (a) Dark-adapted electroretinograms (ERGs) from the two eyes (Eye 1, Eye 2) of a representative *Rpe65*^{-/-} mouse 2 months after a monocular *in utero* subretinal injection of AAV2/1-CMV-*hrRPE65*. ERGs were evoked by increasing intensities of blue light stimuli (stimulus luminance is to the left of key traces). Traces start at stimulus onset. ERG waveforms from Eye 1 are severely abnormal (elevated b-wave threshold of 3–4 log units) and resemble those from uninjected *Rpe65*^{-/-} mice. Eye 2 responses are dramatically different and more like those of an age-matched normal mouse (left column, for comparison). The b-wave threshold is near normal and there are sizeable but abnormal amplitudes; an a-wave can be detected at the brighter intensities. (b) Leading edges of dark-adapted photoresponses (symbols) evoked in the eyes of the *Rpe65*^{-/-} mouse shown in (a); normal photoresponses to the same stimuli are shown on the left. Lines are the model of rod phototransduction activation fitted as an ensemble to the photoresponses. (c and d) Retinal function results from all animals in all groups. For *in utero*-injected animals (left), Eye 1 is defined as the eye with the lower photoresponse sensitivity. Red-filled symbols (“treatment success”) represent those results falling beyond the 99% confidence interval limit (upper boundary of the gray bars) for each parameter determined from uninjected age-matched *Rpe65*^{-/-} mice. Lines connect data obtained from the two eyes of each animal. Many of the Eye 2 group show retinal function that is as good as or better than that in eyes treated postnatally (Tx, right).

FIG. 4. Rhodopsin is present in *Rpe65*^{-/-} mouse retinas treated with AAV2/1-CMV-*hrRPE65*. Absorbance difference spectra of rhodopsin and opsin from Eye 1 and Eye 2 of *in utero*-treated *Rpe65*^{-/-} mice (purple traces) and from eyes of mice treated postnatally (black lines). Rhodopsin–opsin data are shown for animals treated (b) *in utero* or (c) as adults: the abscissa gives the amount of opsin determined for each eye, while the ordinate gives the amount of rhodopsin recovered from the same eye; lines connect the data obtained from the two eyes of each mouse. (c) For animals injected as adults, the rhodopsin–opsin values are compared in control and treated eyes. Many of the samples in the Eye 2 group show rhodopsin–opsin ratios that are as good as or better than those in eyes known to be treated postnatally. The gray bar represents the noise level for detection of the presence of rhodopsin, set by the 95% confidence interval about the mean of the values for the untreated eyes of the mice in the postnatal group (black triangles).

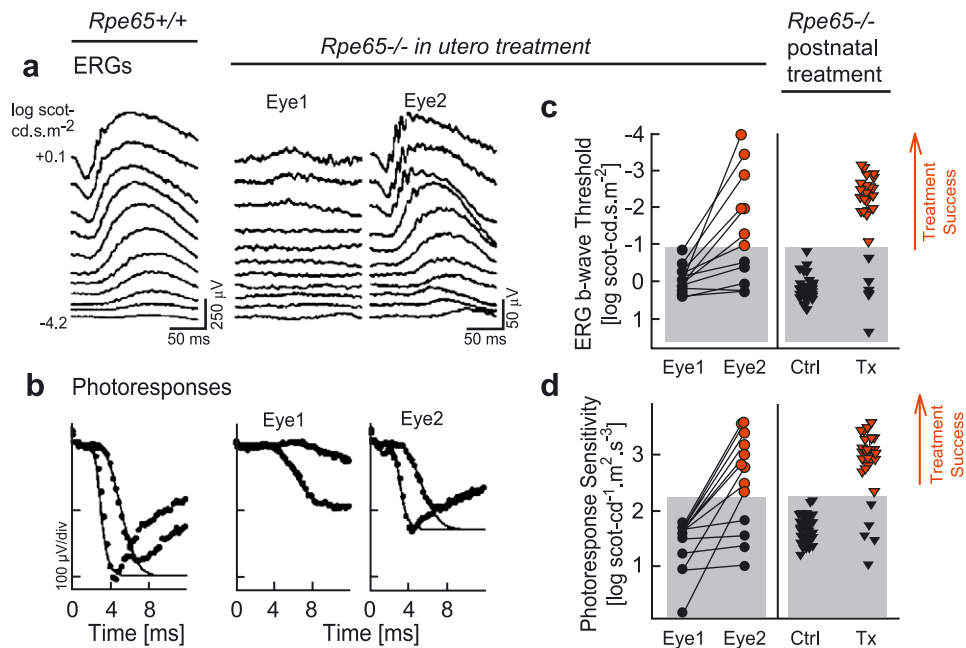


FIG. 3.

$\pm 0.2 \log \text{scot-cd}^{-1} \text{m}^2 \text{s}^{-3}$, $n = 6$). Eye 1, on the other hand, has a very slow photoresponse leading edge (peaking near 10 ms), with a sensitivity of $1.68 \log \text{scot-cd}^{-1} \text{m}^2 \text{s}^{-3}$ (sensitivities for uninjected $Rpe65^{-/-}$ mice, $2.0 \pm 0.3 \log \text{scot-cd}^{-1} \text{m}^2 \text{s}^{-3}$, $n = 8$).

We chose two ERG parameters, ERG b-wave threshold and photoresponse sensitivity, to evaluate efficacy of the gene therapy, considering that $Rpe65$ deficiency causes photoreceptors to be extremely insensitive to light due to a lack of 11-*cis*-retinal chromophore [4]. In animals

injected *in utero*, we did not know the identities of the control and the treated eyes. Therefore, we used ERG results in postnatally treated animals, in which the treatment eye was known, to interpret the results of the *in utero* experiments. For postnatally treated eyes, both ERG parameters were significantly better than in control eyes (ERG b-wave thresholds -1.9 ± 1.2 versus $0.2 \pm 0.3 \log \text{scot-cd s m}^{-2}$, $P < 0.001$; photoresponse sensitivity 2.8 ± 0.6 versus $1.7 \pm 0.3 \log \text{scot-cd}^{-1} \text{m}^2 \text{s}^{-3}$, $P < 0.001$). When “treatment success” was defined as a parameter

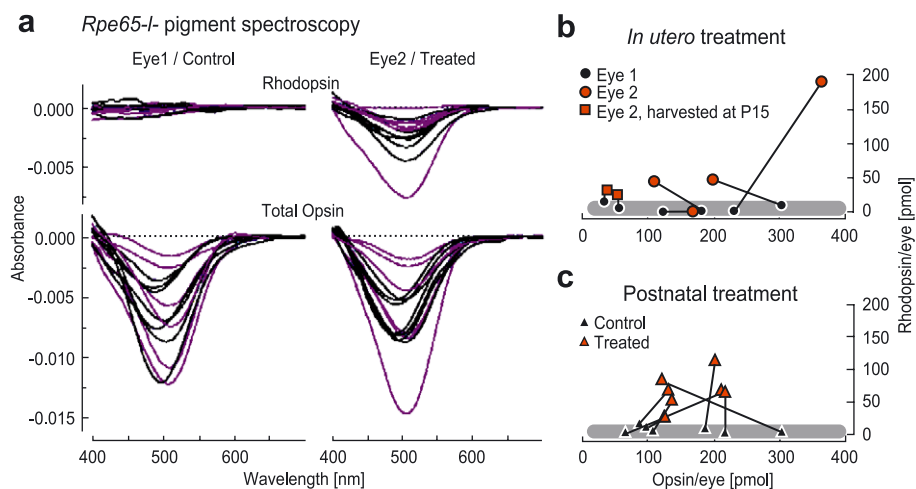


FIG. 4.

value better than the 99% confidence interval of results obtained in age-matched uninjected *Rpe65*^{-/-} eyes, postnatal treatment had an ~80% success rate (Figs. 3c and 3d, red symbols).

For animals treated *in utero*, we ordered the data from the two eyes as follows: the eye with lower photoreponse sensitivity was designated Eye 1 and the eye with higher sensitivity Eye 2. None of the Eye 1 group showed treatment success for either ERG parameter, whereas 54% of the Eye 2 group showed treatment success for ERG b-wave threshold and 70% for photoreponse sensitivity (Figs. 3c and 3d). The ERG parameters were significantly better in the Eye 2 group compared to Eye 1 (ERG b-wave thresholds -1.3 ± 1.5 versus -0.1 ± 0.4 log scot-cd s m⁻², $P = 0.003$; photoreponse sensitivity 2.5 ± 0.9 versus 1.4 ± 0.5 log scot-cd⁻¹ m² s⁻³, $P < 0.001$). In two animals on which we performed both immunocytochemistry and ERGs, the eyes with the greater photoreponse sensitivity showed *Rpe65* expression.

Correction of the Biochemical Defect after *in Utero* AAV2/1-Mediated Retinal Gene Therapy

We also tested the ability of the photoreceptors to generate rhodopsin. We harvested dark-adapted retinas of the *Rpe65*^{-/-} animals injected *in utero* and of control and treated eyes from animals injected as adults. We extracted visual pigment from 4- to 5-month-old mice ($n = 4$) and P15 mice ($n = 2$) that had been treated *in utero* and from 6-month-old adult animals that had been treated at age 2.5 months ($n = 7$). We measured the rhodopsin content of each eye spectrophotometrically in relation to the total amount of opsin. We found significant levels of rhodopsin in both adult and fetal AAV2/1-CMV-*hRPE65*-treated retinas (Fig. 4a). In animals injected *in utero*, we defined Eye 1 and Eye 2 as the eyes with lower or higher rhodopsin content, respectively. We recovered an average of 67 pmol of rhodopsin in Eye 2 of the *in utero*-treated animals, which was comparable to the average value of 57 pmol recovered from animals treated postnatally (Figs. 4b and 4c). We obtained the highest rhodopsin recovery in Eye 2 of a mouse treated as a fetus (190 pmol), a level about two-thirds of that measured in wild-type C57BL/6 mice under the same conditions (297 ± 85 , $n = 84$; Lyubarsky *et al.*, unpublished data (Fig. 4b)). We did not detect rhodopsin in untreated or control-injected adult *Rpe65*^{-/-} retina (Figs. 4a and 4c) or in Eye 1 of the mice treated as fetuses (Figs. 4a and 4b). In four of the animals with *in utero* treatment, we measured both ERGs and rhodopsin levels; in all eight eyes, the results were concordant in terms of treatment success. We also measured the opsin content of the AAV-treated and untreated eyes using *in vitro* regeneration in the presence of excess 11-*cis*-retinal, and the levels in left and right (experimental versus control) eyes were comparable (160 vs 162 pmol; Fig. 4). The ratio of recovered rhodopsin to total opsin in a treated eye is a measure of treatment success: this ratio

was 0.42 for the eyes of the mice treated postnatally and 0.41 for the eyes treated *in utero* in which rhodopsin was identified (Eye 2) (Fig. 4b).

DISCUSSION

In utero somatic gene transfer has been accomplished in different organ systems [10–14] but has been therapeutically successful as yet only in animal models of hemophilia, mucopolysaccharidosis, and epilepsy [10,15–19]. Our results demonstrate rescue of vision, measurable by immunohistochemistry, electrophysiology, and biochemistry, following *in utero* gene transfer in a murine model of a congenital blinding disease. Remarkably, fetal retinal gene transfer does not interfere with transformation of the retina from the undifferentiated retinal progenitor stage to the laminated differentiated structure found in the adult, and the retinal electrophysiology we performed suggests development of normal synaptic connections. Two of the animals with *in utero* treatment showed nearly normal ERGs; one of the two that had visual pigment measurements showed a nearly normal complement of rhodopsin. Success at this level has not been reported to date in any treatment modality of retinal degeneration [20–23]. Rescue of vision was also demonstrated in adult *Rpe65*^{-/-} mice, similar to that previously reported after treatment of canine *RPE65* mutants [20]. Biochemical results (rhodopsin measurements) in the present study provided additional information regarding gene therapy-mediated correction of the phototransduction cycle.

The ability to achieve a therapeutic effect on retinal function after delivery to the adult retina of the murine model of LCA adds generality to the previous success observed in treatment of the retina of the canine model of the same disease [20]. Of course, there are many more steps (ranging from safety studies to discussion of ethical implications) that must be taken before *in utero* gene therapy for human retinal disease becomes a reality. Nevertheless, the results from this study indicate that *in utero* treatment of a congenital blinding disease is indeed possible. In addition, the success reported here after *in utero* gene delivery has important implications for the many retinal diseases that have a strong developmental component or a rapid early postnatal course of retinal degeneration and visual loss [24]. *In utero* treatment could potentially correct the defect before significant organ damage has evolved and could prevent downstream developmental abnormalities of the retina leading from primary photoreceptor and RPE disease [7,25,26]. Congenital retinal disease can cause human visual cortical reorganization [27] and thus raises the concern that abnormal visual experience early in life may frustrate postnatal treatment strategies, making an *in utero* approach attractive. Finally, given the similarities in patterns of differentiation of the retina with the brain, fetal

gene delivery may prove to be an efficient, stable, and safe mode with which to correct developmental defects affecting other portions of the central nervous system.

MATERIALS AND METHODS

Virus preparation (AAV2/1-CMV-hRPE65). RNA was isolated from a human-derived RPE cell line, ARPE19, using TRIZOL reagent (Invitrogen, Carlsbad, CA, USA). The RNA was reverse transcribed using the Superscript Preamplification System for First-Strand cDNA Synthesis (Invitrogen). The target cDNA was amplified via PCR using the components of the Advantage-HF 2 PCR Kit (BD Biosciences Clontech, Palo Alto, CA, USA). Two primers were designed for this purpose. The forward primer encoded a *NotI* end and the first 30 bp of the *hRPE65* cDNA (5'-AAG-GAAAAAGCGCCGCATGTCTATCCAGGTTGAGCATCCTGCTGGT-3'). The reverse primer encoded a *ScaI* end and the last 39 bp of the *hRPE65* cDNA (5'-AAAAGTACTTCAAGATTTTTGAACAGTCCATGAAAGGTGACAGGGAT-3'). PCR product was purified and cloned into the PCR Blunt II TOPO vector using the Zero Blunt TOPO PCR Cloning Kit (Invitrogen). Verification of the identity of the *hRPE65* cDNA was made by DNA sequencing. The cDNA was subsequently excised using *NotI* and *ScaI* and subcloned into pAAV2.1CMV-eGFP3 (provided by J. Wilson, University of Pennsylvania), an AAV vector carrying a CMV promoter and poly(A) tail. The AAV2/1 serotype was selected for its ability to target mainly RPE cells [11]. Virus was prepared by triple transfection and titered, as previously described ($3.9\text{--}6.8 \times 10^{13}$ particles/ml) using a real-time PCR-based assay [28]. In addition, the purity of the virus was assessed by the QCL-1000 Chromogenic Endpoint *Limulus* Amebocyte Lysate assay (BioWhittaker, Inc., Walkersville, MD, USA) to detect endotoxin associated with gram-negative bacteria. The virus preparations used in these studies were free of any significant endotoxin contaminants.

Animals and postnatal virus administration. *Rpe65*^{-/-} mice were generated as described [4]. All procedures were performed in adherence with institutional guidelines and were approved by the Institutional Animal Care and Use Committee. Virus (1 μ l; 5×10^{10} particles) was delivered unilaterally and subretinally to adult mice (1–2.5 months of age) via a transcleral transchoroidal approach. Contralateral eyes received subretinal injection of PBS and served as a control. Animals were maintained for 2–4 months during which time ERGs were performed. Representative eyes were evaluated immunohistochemically for presence of RPE65 protein. Biochemical assays of opsin and rhodopsin levels were performed when animals were 4–6 months of age (3–4 months after injection).

In utero delivery of AAV2/1-CMV-hRPE65. Fetal subretinal injections were performed in pregnant *Rpe65*^{-/-} mice on E14, where E0 was the day on which a vaginal plug was detected. *Ex utero* surgery was performed as described [11]. A midline laparotomy was performed and the uterus was exposed. After the uterus wall was incised, the fetuses were released using cotton swabs. These swabs were also used to control bleeding throughout the surgery. One eye was injected in the two or three fetuses remaining in the uterine horn. Phosphate-buffered saline containing penicillin/streptomycin (PBS/pen/strep; Gibco) was used for lavage of the peritoneum and the exposed fetuses during the surgical procedure. After the uterine wall was incised, one eye of each fetus was injected by inserting a virus-filled glass needle directly through the extraembryonic membrane into the subretinal space. Material (0.1 μ l) was injected through this needle, which had a tip diameter of 15–20 μ m, using a pressure microinjector (Harvard Apparatus, Holliston, MA, USA). To verify the position of the micropipette tip and the accuracy of the injections, the virus was combined with 0.025% (wt/vol) Fast green (Sigma, St. Louis, MO, USA). Accurate subretinal injections could be appreciated by observing a slow spread of the dye from the peripheral injection site throughout the subretinal space. Only one eye was injected in fetuses and the contralateral uninjected eyes served as controls. The eye that was most accessible was injected subretinally. Since it was not possible to mark each fetus according to which eye was injected, histological, biochemical, and functional analyses were used in a

“masked” fashion to identify the treated retinas after birth (see Results). Prior to closing of the abdominal wall, the peritoneum was filled with the PBS/pen/strep solution. The fetuses were delivered by cesarean section on gestational day 19 and fostered to surrogate mothers. ERGs were performed when animals were 1–2 months of age and opsin and rhodopsin measurements made at age 5 months. Representative eyes were evaluated immunohistochemically for presence of RPE65 protein.

Electroretinograms. Our ERG recording methodology in rodents has been described [29]. Briefly, dark-adapted (overnight) animals were anesthetized with an intramuscular injection of a mixture of ketamine HCl (65 mg/kg) and xylazine (5 mg/kg) and pupils were dilated with tropicamide (1%) and phenylephrine (2.5%). Full-field bilateral ERGs were recorded using a custom-built ganzfeld, a computer-based system (EPIC-XL; LKC Technologies, Inc, Gaithersburg, MD, USA), and specially made contact lens electrodes (Hansen Ophthalmics, Iowa City, IA, USA). Medium- and high-energy (10 μ s and 1 ms duration, respectively) flash stimulators (with unattenuated maximal white flash luminances of 0.8 and 3.6 log scot-cd s m⁻², respectively) were used. Neutral density (Wratten 96; Kodak, Rochester, NY, USA) and blue (Wratten 47A) filters served to attenuate and spectrally shape the stimuli. First, dark-adapted ERGs were obtained with increasing intensities (-4.2 to 0.1 log scot-cd s m⁻²) of blue flashes. Next, dark-adapted ERG photoresponses were evoked with two flash intensities (blue 2.2 and white 3.6 log scot-cd s m⁻²). The threshold intensity to evoke a criterion (20 μ V) ERG b-wave response was determined by plotting b-wave amplitudes (measured conventionally from baseline or a-wave trough to positive peak) as a function of stimulus intensity and linearly interpolating the stimulus intensity value that corresponded to the criterion amplitude. Leading edges (4 to 10 ms, depending on the response) of photoresponses were fitted as an ensemble with a model of rod phototransduction activation [30], and maximum amplitude and sensitivity parameters were derived. Paired *t* tests were used to determine the statistical significance of differences between treated and control eyes.

Rhodopsin assay. Individual retinas were harvested and sonicated in the dark in 0.5–1 ml of water. The sonicated homogenate was divided into two aliquots, one for rhodopsin measurement and the other for opsin measurement. To measure rhodopsin, hydroxylamine (Sigma) was added to a final concentration of 10 mM and the differential spectrum after/before illumination was recorded. Spectra were measured using a Lambda 20 spectrophotometer (Perkin–Elmer, Wellesley, MA). The concentration of rhodopsin was obtained from the change in absorbance at 500 nm. To measure regeneration-competent opsin, 11-*cis*-retinal (a gift from Dr. Rosalie Crouch, Medical University of South Carolina) or 9-*cis*-retinal (Sigma), at 10-fold excess of the expected amount of opsin from an average C57BL/6 (wild-type) retina [6], was added to the retinal homogenate and incubated for 30 min at 37°C. This treatment results in reconstitution of either rhodopsin from opsin and 11-*cis*-retinal or isorhodopsin from opsin and 9-*cis*-retinal. Rhodopsin or isorhodopsin concentrations were determined spectrophotometrically as described above. In the case of 9-*cis*-retinal, the change in absorbance at 480 nm was used to quantify the isorhodopsin concentration. The molar extinction coefficients used were 42,000 and 44,000 for rhodopsin and isorhodopsin, respectively [31]. To validate the opsin regeneration protocol, sonicated retinal homogenate from dark-adapted wild-type mice was divided into two aliquots, rhodopsin was measured in one of them, the second aliquot was completely bleached and regeneration-competent opsin was measured as has been outlined. The efficiency of rhodopsin and isorhodopsin reconstitution was >95%. Rhodopsin and opsin were measured in each retina, unless otherwise specified.

Immunohistochemistry. Eyes were enucleated, fixed in 4% paraformaldehyde/PBS overnight, cryoprotected with 30% sucrose/PBS, and embedded in optimal cutting temperature compound (Fisher Scientific, Pittsburgh, PA, USA). A cryostat (Reichert Jung Model 8200, Leica Microsystems, Inc., Wetzlar, Germany) was used to obtain 10- μ m-thick serial sections. RPE65 was labeled with a polyclonal rabbit anti-RPE65 primary antibody (PETLET; 1:200) [4]. This antibody is designed to target an RPE65-specific amino acid sequence found in diverse species. The primary

anti-RPE65 antibody was detected with an anti-rabbit Alexa 468 secondary antibody (1:100; Molecular Probes, Eugene, OR, USA). Sections were evaluated with a Leica DME microscope (Leica Microsystems, Inc.) equipped with epifluorescence and images were captured with a Hamamatsu digital camera and Openlab 2.2 image analysis software (Improvision, Inc., Boston, MA, USA).

ACKNOWLEDGMENTS

This study was supported by NIH U10EY013729 (J.B. and S.G.J.), R01 EY10820 and EY12156 (J.B.), EY13385 (S.G.J.), EY13203 (A.V.C.), F32-EY07065 (N.S.D.), EY02660 (E.N.P.), and 5-P30-DK-47747-10 (Vector Core Facility); the Foundation Fighting Blindness (J.B., S.G.J., A.V.C., T.S.A.); the Lois Pope LIFE Foundation (J.B.); the Macula Vision Research Foundation (S.G.J.); The William and Mary Greve International Research Scholar Award (J.B., A.V.C.); Research to Prevent Blindness, Inc.; the Ruth and Milton Steinbach Fund (J.B.); the Paul and Evanina Mackall Trust; and the F.M. Kirby Foundation. We thank Sergei Nikonov (University of Pennsylvania) for technical assistance.

RECEIVED FOR PUBLICATION OCTOBER 30, 2003; ACCEPTED NOVEMBER 20, 2003.

REFERENCES

1. Cremers, F. P., Van Den Hurk, J. A., and Den Hollander, A. I. (2002). Molecular genetics of Leber congenital amaurosis. *Hum. Mol. Genet.* **11**: 1169–1176.
2. Marlhens, F., et al. (1997). Mutations in RPE65 cause Leber's congenital amaurosis. *Nat. Genet.* **17**: 139–141.
3. Morimura, H., Fishman, G. A., Grover, S. A., Fulton, A. B., Berson, E. L., and Dryja, T. P. (1998). Mutations in the RPE65 gene in patients with autosomal recessive retinitis pigmentosa or Leber congenital amaurosis. *Proc. Natl. Acad. Sci. USA* **95**: 3088–3093.
4. Redmond, T. M., et al. (1998). Rpe65 is necessary for production of 11-cis-vitamin A in the retinal visual cycle. *Nat. Genet.* **20**: 344–351.
5. Manes, G., Leducq, R., Kucharczak, J., Pages, A., Schmitt-Bernard, C. F., and Hamel, C. P. (1998). Rat messenger RNA for the retinal pigment epithelium-specific protein RPE65 gradually accumulates in two weeks from late embryonic days. *FEBS Lett.* **423**: 133–137.
6. Rohrer, B., et al. (2003). Correlation of regenerable opsin with rod ERG signal in Rpe65^{-/-} mice during development and aging. *Invest. Ophthalmol. Visual Sci.* **44**: 310–315.
7. Porto, F. B. O., et al. (2002). Prenatal human ocular degeneration occurs in Leber's congenital amaurosis (LCA2). *J. Gene Med.* **4**: 390–396.
8. Jacobson, S., et al. (2003). Crumbs homologue 1 (CRB1) mutations result in a thick human retina with abnormal lamination. *Hum. Mol. Genet.* **12**: 1073–1078.
9. Lorenz, B., et al. (2000). Early-onset severe rod–cone dystrophy in young children with RPE65 mutations. *Invest. Ophthalmol. Visual Sci.* **41**: 2735–2742.
10. Schneider, H., et al. (2002). Sustained delivery of therapeutic concentrations of human clotting factor IX—a comparison of adenoviral and AAV vectors administered in utero. *J. Gene Med.* **4**: 46–53.
11. Surace, E., et al. (2003). Delivery of adeno-associated viral vectors to the fetal retina: impact of viral capsid proteins on retinal neuronal progenitor transduction. *J. Virol.* **77**: 7957–7963.
12. Sekhon, H., and Larson, J. (1995). In utero gene transfer into the pulmonary epithelium. *Nat. Med.* **1**: 1201–1203.
13. Tarantal, A., et al. (2001). Lentiviral vector gene transfer into fetal rhesus monkeys (Macaca mulatta): lung-targeting approaches. *Mol. Ther.* **4**: 614–621.
14. Porada, C., et al. (1998). In utero gene therapy: transfer and long-term expression of the bacterial neo(r) gene in sheep after direct injection of retroviral vectors into pre-immune fetuses. *Hum. Gene Ther.* **9**: 1571–1585.
15. David, A., et al. (2003). Ultrasound-guided percutaneous delivery of adenoviral vectors encoding the beta-galactosidase and human factor IX genes to early gestation fetal sheep in utero. *Hum. Gene Ther.* **14**: 353–364.
16. Waddington, S., et al. (2003). In utero gene transfer of human factor IX to fetal mice can induce postnatal tolerance of the exogenous clotting factor. *Blood* **15**: 1359–1366.
17. Ogawara, M., Takahashi, M., Shimizu, T., Nakajima, M., Setoguchi, Y., and Shirasawa, T. (2002). Adenoviral expression of protein-L-isoaspartyl methyltransferase (PIMT) partially attenuates the biochemical changes in PIMT-deficient mice. *J. Neurosci. Res.* **69**: 353–361.
18. Lipshutz, G., Sarkar, R., Flebbe-Rehwaldt, L., Kazazian, H., and Gaensler, K. (1999). Short-term correction of factor VIII deficiency in a murine model of hemophilia A after delivery of adenovirus murine factor VIII in utero. *Proc. Natl. Acad. Sci. USA* **96**: 13324–13329.
19. Meertens, L., et al. (2002). In utero injection of alpha-L-iduronidase-carrying retrovirus in canine mucopolysaccharidosis type I: infection of multiple tissues and neonatal gene expression. *Hum. Gene Ther.* **13**: 1809–1820.
20. Acland, G. M., et al. (2001). Gene therapy restores vision in a canine model of childhood blindness. *Nat. Genet.* **28**: 92–95.
21. Narstrom, K., et al. (2003). Functional and structural recovery of the retina after gene therapy in the RPE65 Null mutation dog. *Invest. Ophthalmol. Visual Sci.* **44**: 1663–1672.
22. Van Hooser, J. P., et al. (2000). Rapid restoration of visual pigment and function with oral retinoid in a mouse model of childhood blindness. *Proc. Natl. Acad. Sci. USA* **97**: 8623–8628.
23. Dejneka N. S., Rex T. S., and Bennett J. (Eds.). (2003). *Gene Therapy and Animal Models for Retinal Disease* (pp. 188–198). Basel: Karger.
24. Weleber, R. (2002). Infantile and childhood retinal blindness: a molecular perspective. *Ophthalmic Genet.* **23**: 71–97.
25. Banin, E., et al. (1999). Retinal rod photoreceptor-specific gene mutation perturbs cone pathway development. *Neuron* **23**: 549–557.
26. Jones, B. E., et al. (2003). Retinal remodeling triggered by photoreceptor degenerations. *J. Comp. Neurol.* **464**: 1–16.
27. Baseler, H., Brewer, A., Sharpe, L. T., Morland, A., Jagle, H., and Wandell, B. (2002). Reorganization of human cortical maps caused by inherited photoreceptor abnormalities. *Nat. Neurosci.* **5**: 364–370.
28. Hildinger, M., Auricchio, A., Gao, G., Wang, L., Chirmule, N., and Wilson, J. (2001). Hybrid vectors based on adeno-associated virus serotypes 2 and 5 for muscle-directed gene transfer. *J. Virol.* **75**: 6199–6203.
29. Aleman, T., et al. (2001). Augmented rod bipolar cell function in partial receptor loss: an ERG study in P23H rhodopsin transgenic and normal rats. *Vision Res.* **41**: 2779–2797.
30. Cideciyan, A., and Jacobson, S. (2001). An alternative phototransduction model for human rod and cone ERG a-waves: normal parameters and variation with age. *Vision Res.* **36**: 2609–2621.
31. Crouch, R., Purvin, V., Nakanishi, K., and Ebry, T. (1996). Isorhodopsin II: artificial photosensitive pigment formed from 9,13-dicis retinal. *Proc. Natl. Acad. Sci. USA* **72**: 1538–1542.